Cram, R. Jaeger, K. Deshayes, *J. Am. Chem. Soc.* **115**, 10111 (1993); D. J. Cram, *Nature* **356**, 29 (1992); M. Fujita, N. Satoshi, K. Ogura, *J. Am. Chem. Soc.* **117**, 1649 (1995).
4. The assembly was modeled on a Silicon Graphics Personal Iris with Macromodel V3.5X, MM2 force field with the GB/SA model [F. Mohamadi *et al.*, *J. Comput. Chem.* **11**, 440 (1990)].
5. For similar reactions of *tert*-butyl hydrazodiformate, see L. A. Carpino, *J. Am. Chem. Soc.* **85**, 2144 (1963).
6. The synthesis follows that of a related tetramethyl ester [R. Beerli and J. Rebek Jr., *Tetrahedron Lett.* **36**, 1813 (1995)].
7. Introduction of the 1,3-adamantanedicarboxylic acid to the NMR tube followed by vigorous shaking for 10 s is all that is necessary to cause dissolution.
8. In the cases of the 1-adamantaneamine and 1-adamantanecarboxylic acid (Fig. 5B), the proton resonances of nonencapsulated guests are discernable in the region between 1 and 2 ppm and can be estimated to be about equal in intensity to the resonances of the included guest. For 1,3,5,7-tetramethyladamantane (Fig. 5E), the proton resonances of the nonencapsulated guest are the very large peaks whose bases are visible at 0.8 ppm; at full scale, these resonances are about 60 times as intense as the resonances of the included guest. This guest can be displaced by the addition of 20 equivalents of benzene for each equivalent of 1,3,5,7-tetramethyladamantane, indicating that benzene, by comparison, is a much less favored guest.
9. H. Dugas, *Bioorganic Chemistry* (Springer-Verlag, New York, ed. 2, 1989), pp. 20–21.
10. The value for the complex term [**1b** · guest · **1b**] was measured from the NMR spectra by using an internal standard, and the [$\mathbf{1b}_{(aggregate)}$] and [guest] values were calculated by subtracting the complex amount from the total amounts. Several assumptions were made: (i) the amount of dimer (unfilled or filled with solvent) present before addition of the guest is negligible, (ii) after addition of the guest, all the host material not assembled into the complex is in the aggregate state, and (iii) the association of the guest with itself is negligible.
11. R.S.M. thanks NIH for a fellowship, and we thank NIH for support of this research.

2 June 1995; accepted 22 August 1995

Yeast Checkpoint Genes in DNA Damage Processing: Implications for Repair and Arrest

David Lydall and Ted Weinert

Yeast checkpoint control genes were found to affect processing of DNA damage as well as cell cycle arrest. An assay that measures DNA damage processing in vivo showed that the checkpoint genes *RAD17, RAD24*, and *MEC3* activated an exonuclease that degrades DNA. The degradation is probably a direct consequence of checkpoint protein function, because *RAD17* encodes a putative 3′-5′ DNA exonuclease. Another checkpoint gene, *RAD9*, had a different role: It inhibited the degradation by *RAD17*, *RAD24*, and *MEC3*. A model of how processing of DNA damage may be linked to both DNA repair and cell cycle arrest is proposed.

Checkpoint controls recognize DNA damage and halt cell division until DNA repair is complete. They are thought to play an important role in tumor prevention, because human checkpoint genes, such as *p53* and *ATM*, are often compromised in tumor cells (*1*). How eukaryotic checkpoint controls work to sense DNA damage and to signal arrest is unclear. Studies in yeasts have identified genes that are essential for arrest in G_2 after DNA damage, at the G_2 checkpoint. Here we examine the role of the G_2 checkpoint genes *RAD9*, *RAD17*, *RAD24*, and *MEC3* (*2–5*) in yeast. Other genes, *MEC1*, *RAD53*, and *POLε*, are also required for checkpoint control at the S-phase checkpoint when DNA replication is blocked (*5–7*).

Department of Molecular and Cellular Biology, University of Arizona, Tucson AZ 85721, USA.

Checkpoint proteins could be involved in a signal transduction pathway linking DNA damage to cell cycle arrest. However, several observations suggested to us that the *RAD9*, *RAD17*, *RAD24*, and *MEC3* genes are not solely, if at all, involved in signal transduction. We found that these four checkpoint control genes can be divided into two groups based on phenotypes that suggest possible roles in DNA repair. These groups are the *RAD24* group (*RAD17*, *MEC3*, and *RAD24*) and the *RAD9* group (consisting only of the *RAD9* gene) (Table 1). We found, for example, that *rad9 rad24* double mutants are more sensitive to the DNA damage caused by ultraviolet (UV) radiation and methyl methane sulfonate (MMS) than are the corresponding single mutants (Fig. 1). Our analysis of the results summarized in Table 1 led us to test whether the *RAD9* and *RAD24* group genes

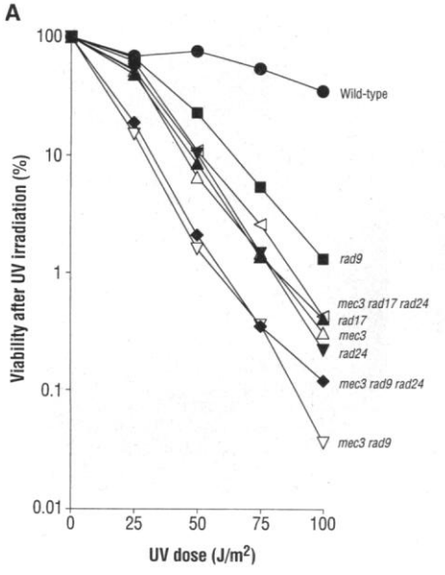

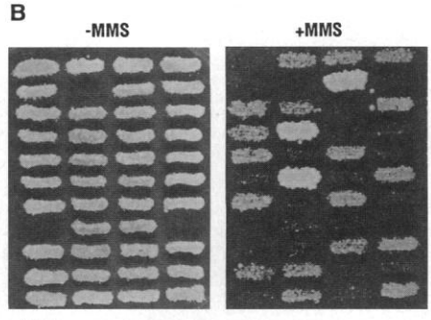

Tetrad number	a	b	c	d
1	9, 17	9	3, 17, 24	3, 24
2	3, 9	–	WT	3, 9, 17, 24
3	3, 17, 24	9	3, 9, 24	17
4	24	WT	3, 9, 17	3, 9, 17, 24
5	24	9, 17, 24	3, 17	3, 9
6	3, 9, 24	WT	9, 17, 24	3, 17
7	17, 24	3, 9	3, 17	9, 24
8	–	9, 17, 24	9, 24	–
9	3, 9, 24	9, 17	3, 24	17
10	3	3, 17, 24	9, 17	9, 24
11	3, 9, 24	3	9, 17, 24	17

Fig 1. Assignment of *rad9* mutants to a different epistasis group than *rad17*, *rad24*, and *mec3* mutants. (**A**) Sensitivity of checkpoint mutant strains to UV irradiation. A series of A364a strains in which combinations of the *RAD9, RAD17, RAD24*, and *MEC3* genes had been deleted were tested for their sensitivity to UV irradiation. All the survival curves shown were obtained on the same day. There was slight day-to-day variation in cell viability, but whenever a *rad9* mutation was combined with any other checkpoint mutation the cells were more sensitive to UV irradiation. Experiments in the W303 background produced a similar pattern (*16*). (**B**) Sensitivity of checkpoint mutant strains to the alkylating agent MMS. Strain DLY 217 (A364a background, *Mat**a** rad9::HIS3 rad17::LEU2 rad24::TRP1 mec3::URA3*) was crossed to strain DLY221 (A364a background, *Matα his3 leu2 trp1 ura3*). The diploid was sporulated, and all possible combinations of mutations were found in the haploid progeny. Strains were replica-plated to YEPD-rich plates (containing yeast extract, peptone, and dextrose) with (+) or without (−) 0.01% MMS. In addition, the progeny from each tetrad (labeled a, b, c, or d in table) were replica-plated to −URA, −HIS, −LEU, and −TRP plates to determine which checkpoint mutations were present. Abbreviations in table are as follows: 3, *mec3::URA3*; 9, *rad9::HIS3*; 17, *rad17::LEU2*; 24, *rad24::TRP1*; and WT, wild type. A dash indicates that this particular spore did not grow. Three levels of growth were observed in the presence of MMS: Wild-type cells were MMS-resistant, *rad9* or *rad24* group mutants were sensitive, and *rad9 rad24* group double mutants were supersensitive. Consistent results were found in the W303 genetic background (*16*).

have different roles in DNA repair. In addition, *rad9* and *rad24* group mutants had different viabilities after meiosis and after the *CDC13* DNA replication gene was inactivated (Table 1 and Fig. 2).

To study the role of checkpoint genes in DNA repair we needed a way to measure DNA repair in vivo. Garvik *et al.* have recently characterized the type of damage formed in temperature-sensitive *cdc13* mutants (*8*). They have shown that *cdc13* strains generate telomere-proximal DNA damage at 36°C in which the TG strand becomes single-stranded (ss) because the AC strand is lost. Centromere-proximal DNA sequences remain intact. *CDC13* is therefore thought to have a specific role in the replication of the ends of chromosomes. We were encouraged to assay *cdc13*-induced DNA damage because both *RAD9* and *RAD24* are needed for cell cycle arrest of *cdc13* mutants. We suspected that *rad9* and *rad24* mutants might process *cdc13*-induced damage differently because, although both strains are equally checkpoint-defective, *cdc13 rad9* strains lose viability more rapidly than do *cdc13 rad24* mutants (Table 1 and Fig. 2E). We thought that the differences in viability might reflect differences in damage processing.

To assay DNA damage processing in *cdc13* mutants, we measured the amount of ss DNA that accumulated at a single copy sequence near the telomere of chromosome V during a single cell cycle (Fig. 2A). Cells began in G_1 and proceeded synchronously through S and G_2 before arresting in late mitosis (Fig. 2, B and C). We harvested cells during the experiment to analyze their DNA. We found that RAD^+, *rad24*, and *rad9* cells processed *cdc13*-induced DNA damage with very different kinetics (Fig. 2D). In the checkpoint-proficient RAD^+ cells, ss DNA first appeared after cells had completed DNA replication and while they were arrested in G_2. In contrast, *rad24* mutants failed to accumulate ss DNA until long after they had passed the G_2-M checkpoint. *rad9* mutants had yet another phenotype and accumulated ss DNA damage even earlier than did RAD^+ cells. This experiment allowed us to draw several conclusions. First, the ss DNA observed in *cdc13* RAD^+cells is not due to incomplete DNA replication per se, but rather is largely a consequence of *RAD24*-mediated DNA degradation. Second, *RAD9* seems to be able to inhibit the *RAD24*-dependent degradation. The idea that *RAD9* inhibits a *RAD24*-dependent

Table 1. Mutants of the *rad9* and *rad24* groups show different phenotypes. Double mutants of the *rad9 rad24* group were more sensitive to UV- and MMS-induced DNA damage than was either single mutant (Fig. 1). R, resistant; S, sensitive; SS, supersensitive. The *rad9* diploids produced viable spores, but *rad24* group diploids showed low spore viabilities. The *cdc13 rad9* mutants died more rapidly than did the *cdc13 rad24* mutants (cell viabilities after 4 hours at 36°C in the type of experiment shown in Fig. 2 are given). Previously published results show that *cdc13 rad17* and *cdc13 mec3* mutants behave like *cdc13 rad24* mutants (*3, 5*). All experiments used checkpoint gene disruptions (*2*). ND, not determined.

Mutants	UV or MMS damage	Spore viability (%)	Viability with *cdc13* (%)
RAD+	R	90	93 ± 18.1
rad9	S	92	0.6 ± 0.33
rad24	S	9	43 ± 13.3
rad17	S	22	ND
mec3	S	20	ND
rad9 rad24	SS	ND	25 ± 2.9

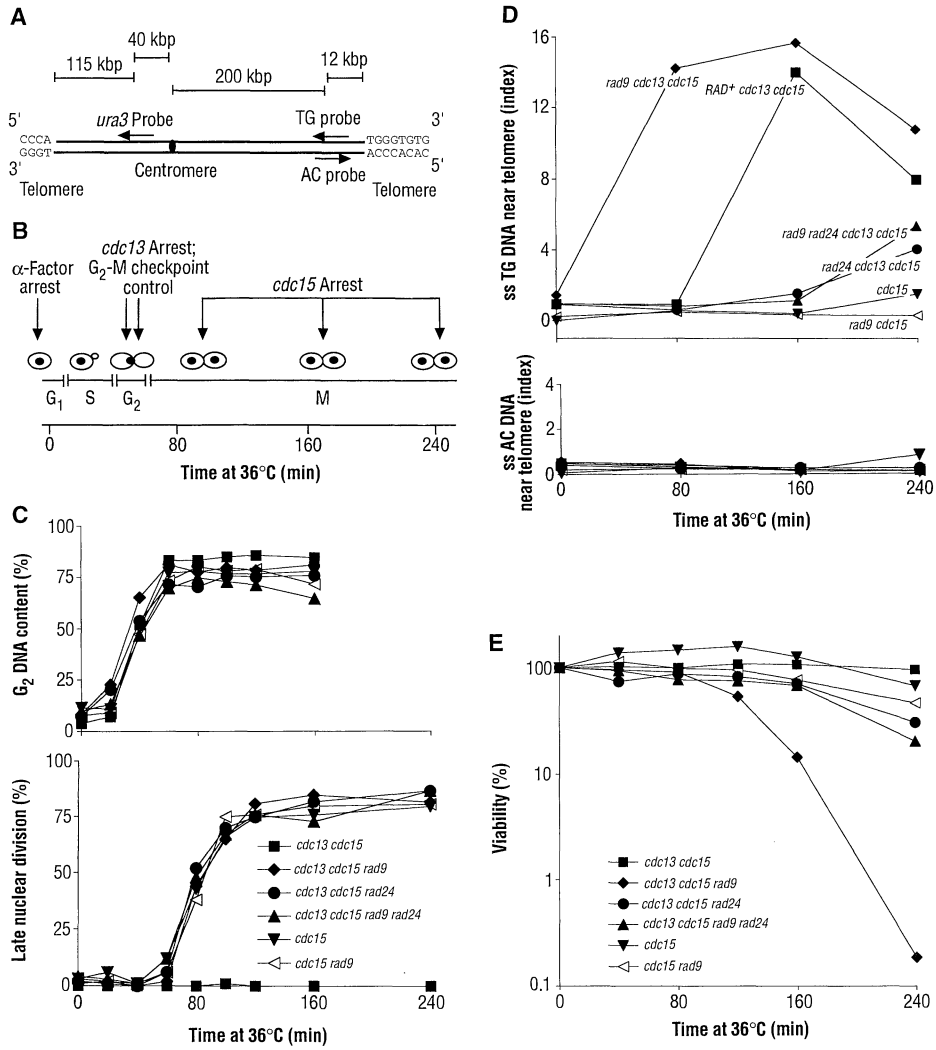

Fig. 2. Effect of checkpoint genes on DNA metabolism in *cdc13* mutants. (**A**) Physical map of chromosome V (*17*). (**B**) Strategy used to synchronize *cdc13* cultures. Strains were arrested in G_1 by the addition of α-factor (20 nM for 2.5 hours at 23°C). The α-factor was removed by centrifugation, and the temperature of the cultures was changed to 36°C to inactivate *cdc13* and *cdc15*. Thereafter, samples were removed to determine the DNA content (by flow cytometry), cell cycle position (by 4′,6′-diamidino-2-phenylindole staining of DNA and fluorescence microscopy), and cell viability (by counting of colonies after 3 days of growth at 23°C). The bulk of the culture was harvested and frozen for subsequent DNA extraction. (**C**) Top panel shows the percentage of cells that contained G_2 DNA. Bottom panel shows the percentage of cells in late nuclear division. The relevant genotypes for strains were as follows: DLY408, squares (*cdc13-1 cdc15-2*); DLY409, diamonds (*cdc13-1 cdc15-2 rad9::HIS3*); DLY410, circles (*cdc13-1 cdc15-2 rad24::TRP1*); DLY411, solid upward-pointing triangles (*cdc13-1 cdc15-2 rad9:HIS3 rad24::TRP1*); DLY418, solid downward-pointing triangles (*cdc15-2*); and DLY419, open triangles (*cdc15-2 rad9::HIS3*). (**D**) Single-stranded DNA accumulation in *cdc13* strains. Symbols are the same as in (C). We determined the ss index by measuring the amount of ss DNA present in nondenatured DNA samples in comparison with a denatured loading control (at the URA3 locus) (*18*). The data shown are the mean of four experiments. Analysis of a DNA sequence 30 kbp closer to the centromere than the locus shown in Fig. 2D revealed similar trends; the ss DNA that accumulated was strand-specific, and *rad9* mutants accumulated it more quickly than did *rad24* mutants (*16*). (**E**) Cell viability.

function is supported by the behavior of *rad9 rad24* double mutants; they degrade DNA as slowly as do *rad24* single mutants (Fig. 2D).

These results also suggest that the death of *rad9 cdc13* mutants is not due to the checkpoint defect, as we had previously supposed (*5*). Rather, death is a consequence of DNA degradation controlled by *RAD24*, because the viability of *cdc13 rad9 rad24* mutants is high, whereas that of *cdc13 rad9 RAD24* mutants is low (Fig. 2E). Therefore, in *cdc13 rad9* cells, *RAD24* induces cell death, or suicide, rather than cell cycle arrest.

Our analyses of damage processing suggest that *RAD24* controls an exonuclease that degrades DNA and that *RAD9* counteracts or inhibits this degradation (Fig. 3). The effects of checkpoint proteins on DNA damage processing are probably direct, because we found that *RAD17*, a member of the *RAD24* group, encodes a putative 3′-5′ DNA exonuclease (Fig. 4). Rad17p is similar to the evolutionarily conserved checkpoint and repair proteins Rec1p (*Ustilago maydis*) and Rad1p (*Schizosaccharomyces pombe*) (Fig. 4).

The idea that *RAD9* and *RAD24* have different roles in processing DNA damage may explain the enhanced sensitivity of double mutants to UV- and MMS-induced DNA damage (Fig. 1). The precise roles of *RAD9* and *RAD24* in the repair of different types of DNA damage are, however, unclear. The two genes act in opposition in one pathway of repair after *cdc13*-induced damage, whereas after UV- and MMS-induced damage they appear to act in different pathways of repair (Fig. 1). In addition, we have yet to understand the problem of why the Rad17p 3′-5′ putative exonuclease is required for cell cycle arrest after DNA damage that leaves a 3′ overhang (*9*).

How is processing of DNA damage linked to cell cycle arrest? We suggest that DNA degradation by Rad17p and Rad24p could generate an intermediate in recombinational repair. We suggest two possible causes of cell cycle arrest: Either the processing of damage by checkpoint control proteins sends the signal for arrest [for example, as a result of an allosteric effect caused by DNA binding (Fig. 3, large box)], or the processing of damage generates a DNA structure that sends the signal for arrest (Fig. 3, small box). In either model, other checkpoint proteins (such as Mec1p and Rad53p) may mediate arrest. We must also consider a third possibility, that processing and arrest may be entirely separate activities of checkpoint control proteins, as appears to be the case for the cyclin-dependent kinase inhibitor p21 (*10*).

The bacterial SOS response to DNA damage provides precedence for the link between DNA damage processing and cell cycle arrest. In *Escherichia coli*, ss DNA generated by damage processing activates RecA to signal the SOS response (*11*). For example, double-stranded breaks must be processed by the recBC helicase-exonuclease and pyrimi-

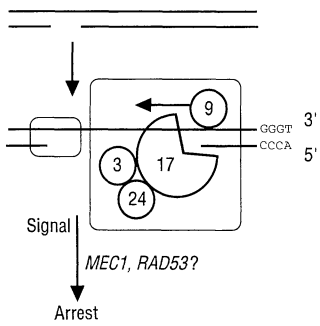

Fig. 3. Model of the role of checkpoint control proteins in *cdc13*-induced DNA damage processing. According to this model, *cdc13* mutants accumulate a small amount of DNA damage during DNA replication at 36°C. Checkpoint control proteins recognize the DNA damage and initiate DNA damage processing. Rad17p (17), Rad24p (24), and Mec3p (3) activate an exonuclease that degrades the AC strand of DNA near telomeres. Rad9p (9) might act as a direct inhibitor of the exonuclease or counteract the exonuclease, for example, by activating a polymerase. *MEC1* and *RAD53* are also required for cell cycle arrest after *cdc13*-induced DNA damage (see text for further details).

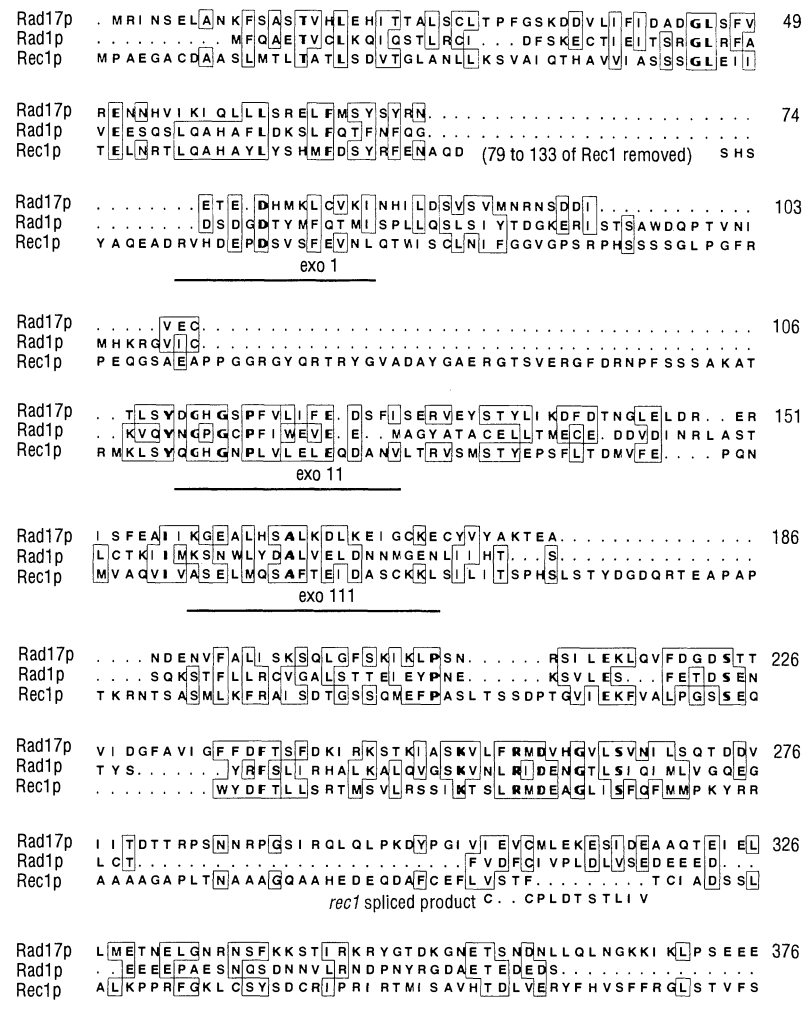

Fig. 4. Comparison of Rad17p, Rad1p, and Rec1p (*19*). *Schizosaccharomyces pombe* Rad1p is 23.2% identical and 50.3% similar to Rad17p. *Ustilago maydis* Rec1p is 21.1% identical and 44.2% similar, and the spliced version is 16.2% identical and 38.2% similar to Rad17p. The three exonuclease domains of 3′-5′ exonucleases, as previously defined (*20*, *21*) and aligned to Rec1p (*22*), are highlighted. These domains are well conserved among Rad17p, Rad1p, and Rec1p, which suggests that all three are 3′-5′ exonucleases (*20–22*). *rad1*$^+$ and *rec1* are each checkpoint control genes, which suggests that evolutionarily conserved proteins link DNA repair to cell cycle arrest (*13*, *23–26*). Dots indicate gaps in the sequence. Amino acids 79 to 113 of Rec1 were deleted in the alignment shown because they did not align to either Rad17p or Rad1p. The numbers on the right refer to the Rad17p sequence. The *rec1* transcript is spliced to make the cDNA product (*24*).

dine dimers must be replicated so that they may generate the ss DNA to activate recA (*12*).

We suggest that other eukaryotic checkpoint control proteins may also participate in DNA damage processing. For example, S-phase checkpoint control may require different proteins to process the type of DNA damage that is induced after DNA replication is inhibited. *POLε* is required for S but not for G_2 checkpoint control (*7*); perhaps this is because *POLε* is specifically required for processing after DNA replication is disturbed. Differences in processing may explain the perplexing patterns of checkpoint gene requirements among species. For example, *rad1*$^+$ and *RAD17* in fission and budding yeasts encode putative 3′-5′ exonucleases and both are required for the G_2 checkpoint in their respective cell types (Fig. 4). However, *rad1*$^+$, yet not *RAD17*, is also required at the S-phase checkpoint (*13*). Similarly, *cdc2*$^+$ and *CDC28* in fission and budding yeasts encode conserved protein kinases. *cdc2*$^+$, yet not *CDC28*, is needed for S-phase checkpoint control (*14*). Perhaps *rad1*$^+$ and *cdc2*$^+$ in fission yeast are required for DNA damage processing after S-phase inhibition, but their homologs in budding yeast are not.

REFERENCES AND NOTES

1. R. Nowak, *Science* **268**, 1700 (1995); K. Savitsky *et al.*, *ibid.*, p. 1749; M. B. Kastan, O. Onyekwere, D. Sidransky, B. Vogelstein, R. W. Craig, *Cancer Res.* **51**, 6304 (1991); S. J. Kuerbitz, B. S. Plunkett, W. V. Walsh, M. B. Kastan, *Proc. Natl. Acad. Sci. U.S.A.* **89**, 7491 (1992).
2. D. Lydall and T. Weinert, in preparation.
3. T. A. Weinert and L. H. Hartwell, *Genetics* **134**, 63 (1993).
4. ———, *Science* **241**, 317 (1988).
5. T. A. Weinert, G. L. Kiser, L. H. Hartwell, *Genes Dev.* **8**, 652 (1994).
6. J. B. Allen, Z. Zhou, W. Siede, E. C. Friedberg, S. J. Elledge, *ibid.*, p. 2401.
7. T. A. Navas, Z. Zhou, S. J. Elledge, *Cell* **80**, 29 (1995).
8. B. Garvik, M. Carson, L. Hartwell, *Mol. Cell. Biol.* **15**, 6128 (1995).
9. Two breaks that cause checkpoint-mediated arrest—an HO endonuclease–induced break during mitosis (*15*) (S. Kim and T. Weinert, unpublished data) and double strand breaks produced during meiosis (D. Lydall and T. Weinert, unpublished data)—both become processed to give a 3′ overhang (implying degradation by a 5′-3′ exonuclease). How a putative 3′-5′ exonuclease (Rad17p) mediates arrest, and perhaps processing, at these two breaks is unclear.
10. R. Li, S. Waga, G. J. Hannon, D. Beach, B. Stillman, *Nature* **371**, 534 (1994).
11. E. M. Witkin, *Biochimie* **73**, 133 (1991).
12. M. Sassanfar and J. W. Roberts, *J. Mol. Biol.* **212**, 79 (1990).
13. T. Enoch, A. M. Carr, P. Nurse, *Genes Dev.* **6**, 2035 (1992); F. Al-Khodairy and A. M. Carr, *EMBO J.* **11**, 1343 (1992); R. Rowley, S. Subramani, P. G. Young, *ibid.*, p. 1335.
14. T. Enoch and P. Nurse, *Cell* **60**, 665 (1990); P. K. Sorger and A. W. Murray, *Nature* **355**, 365 (1992); A. Amon, U. Surana, I. Muroff, K. Nasmyth, *ibid.*, p. 368.
15. L. L. Sandell and V. A. Zakian, *Cell* **75**, 729 (1993).
16. D. Lydall and T. Weinert, data not shown.
17. L. Riles *et al.*, *Genetics* **134**, 81 (1993).
18. Yeast strains used were *MAT***a** *bar1::hisG ade2-1 can1-100 cdc15-2 ura3 leu2-3,112 his3-11 trp1-1* and contained various combinations of *cdc13-1*, *rad9::HIS3*, and *rad24::TRP1*. The *bar1* mutation was present to ensure that G_1 arrest was efficient. The *cdc15-2* mutation was present to ensure that checkpoint control mutants replicated their DNA only once. At 36°C, *cdc15* mutants initiate anaphase but are unable to complete nuclear division. We modified the method of Garvik *et al.* and cut purified yeast DNA with Eco RI before applying the DNA to a slot blot apparatus (*8*). Different filters were probed with GT, AC (from pHR85-31), and *URA3* ss RNA probes. Eco RI was necessary because in some experiments ss DNA was present in a non–strand- and non–locus-specific fashion. This ss DNA did not depend on the presence or absence of *CDC13*. Our interpretation is that it represented replication forks moving through the chromosome. This inconsistent *cdc13*-independent signal disappeared after cutting of the DNA with Eco RI, presumably because the chance that a replication fork was attached to the locus we were probing was reduced. After cutting with Eco RI, most (>95%) of the DNA did not bind to the filter, even after it was denatured. We assume this was because smaller fragments of DNA bind the filter less efficiently. The ss DNA index increased for two reasons. First, ss DNA is created in vivo. Second, as ss DNA is created, Eco RI sites are destroyed, so that the size of the ss DNA increased and it bound the nylon membrane more efficiently. Therefore we cannot make quantitative deductions about the amount of ss DNA produced.
19. Single-letter abbreviations for the amino acid residues are as follows: A, Ala; C, Cys; D, Asp; E, Glu; F, Phe; G, Gly; H, His; I, Ile; K, Lys; L, Leu; M, Met; N, Asn; P, Pro; Q, Gln; R, Arg; S, Ser; T, Thr; V, Val; W, Trp; and Y, Tyr.
20. L. Blanco, A. Bernad, M. Salas, *Gene* **112**, 139 (1992).
21. A. Bernad, L. Blanco, J. M. Lazaro, G. Martin, M. Salas, *Cell* **59**, 219 (1989).
22. M. P. Thelen, K. Onel, W. K. Holloman, *J. Biol. Chem.* **269**, 747 (1994).
23. R. Holliday, R. E. Halliwell, M. W. Evans, V. Rowell, *Genet. Res.* **27**, 413 (1976).
24. K. Onel, M. P. Thelen, D. O. Ferguson, R. L. Bennett, W. K. Holloman, *Mol. Cell. Biol.* **15**, 5329 (1995).
25. K. Onel, R. L. Bennett, P. Unrau, A. Koff, W. K. Holloman, in preparation.
26. A. Nasim and B. P. Smith, *Genetics* **79**, 573 (1975).

27. We thank B. Garvik and L. Hartwell for invaluable discussions and advice about the *cdc13* defect; N. Seaver for help with flow cytometry; A. Adams, L. Hatfield, and M. Ramaswami for criticizing the manuscript; and all the yeasty boys and girls in Tucson for input. D.L. thanks E. Ayres for encouragement. Supported by grants to T.W. from NIH (GM 45276-01), the American Cancer Society, and the March of Dimes foundation.

27 June 1995; accepted 27 September 1995

Activation of the Estrogen Receptor Through Phosphorylation by Mitogen-Activated Protein Kinase

Shigeaki Kato, Hideki Endoh, Yoshikazu Masuhiro, Takuya Kitamoto, Shimami Uchiyama, Haruna Sasaki, Shoichi Masushige, Yukiko Gotoh, Eisuke Nishida, Hiroyuki Kawashima, Daniel Metzger, Pierre Chambon*

The phosphorylation of the human estrogen receptor (ER) serine residue at position 118 is required for full activity of the ER activation function 1 (AF-1). This Ser^{118} is phosphorylated by mitogen-activated protein kinase (MAPK) in vitro and in cells treated with epidermal growth factor (EGF) and insulin-like growth factor (IGF) in vivo. Overexpression of MAPK kinase (MAPKK) or of the guanine nucleotide binding protein Ras, both of which activate MAPK, enhanced estrogen-induced and antiestrogen (tamoxifen)-induced transcriptional activity of wild-type ER, but not that of a mutant ER with an alanine in place of Ser^{118}. Thus, the activity of the amino-terminal AF-1 of the ER is modulated by the phosphorylation of Ser^{118} through the Ras-MAPK cascade of the growth factor signaling pathways.

The ER belongs to a superfamily of ligand-inducible transcription factors that includes receptors for steroid hormones, thyroid hormones, vitamin D_3, and retinoic acid, as well as peroxisome proliferator–activated receptors and orphan receptors (*1*). The ER has two transcriptional activation functions, AF-1 and AF-2, which are located in the NH_2-terminal A/B region and in the ligand-binding domain (region E), respectively (*2*–*6*). Like other steroid hormone receptors, the ER is phosphorylated (*7*–*9*). The ER becomes phosphorylated at several sites when transfected COS-1 cells are treated with estradiol (E_2), and Ser^{118}—the main residue in the A/B region to be phosphorylated (*7*, *8*)—is required for full activity of AF-1 (*7*). The five amino acids located around Ser^{118} (PQLSP) (Fig. 1) (*7*, *10*) are conserved among vertebrate species

S. Kato, Y. Masuhiro, T. Kitamoto, S. Uchiyama, H. Sasaki, S. Masushige, Department of Agricultural Chemistry, Tokyo University of Agriculture, Setagayaku, Tokyo 156, Japan.
H. Endoh and H. Kawashima, Molecular Medicine Research Laboratory II, Yamanouchi Institute for Drug Discovery Research Co. Ltd., Tsukuba, Ibaraki 305, Japan.
Y. Gotoh and E. Nishida, Institute for Virus Research, Kyoto University, Sakyo-ku, Kyoto 606, Japan.
D. Metzger and P. Chambon, Institut de Génétique et de Biologie Moléculaire et Cellulaire, Centre National de la Recherche Scientifique (CNRS)/Institut National de la Santé et de la Recherche Médicale (INSERM)/Université Louis Pasteur/Collège de France, BP163-67404 Illkirch Cedex, Communauté Urbaine de Strasbourg, France.

*To whom correspondence should be addressed.